ELSEVIER

Contents lists available at ScienceDirect

### Journal of Chemical Neuroanatomy

journal homepage: www.elsevier.com/locate/jchemneu



# Amyloid- $\beta$ (25–35) regulates neuronal damage and memory loss via SIRT1/Nrf2 in the cortex of mice



Lin Zhu <sup>a,b,c</sup>, Fangjin Lu <sup>d</sup>, Xiaoyu Jia <sup>a</sup>, Qiuying Yan <sup>a</sup>, Xiaoran Zhang <sup>a</sup>, Ping Mu <sup>a,b,c</sup>, \*

- a Department of Biochemistry and Molecular Biology, Shenyang Medical College, 146 Huanghe North Street, Yuhong District, Shenyang, Liaoning, 110034, People's
- Republic of China

  b Center for Precision Medicine, Shenyang Medical Colleges, 146 Huanghe North Street, Yuhong District, Shenyang, Liaoning, 110034, People's Republic of China
- <sup>c</sup> Key Laboratory of Environment Pollution and Microecology, Shenyang Medical Colleges, 146 Huanghe North Street, Yuhong District, Shenyang, Liaoning, 110034, People's Republic of China
- d Department of Pharmacology, Shenyang Medical Colleges, 146 Huanghe North Street, Yuhong District, Shenyang, Liaoning, 110034, People's Republic of China

#### ARTICLE INFO

#### Keywords: Alzheimer's disease Amyloid-β Neuron Mitochondrion SIRT1

#### ABSTRACT

Alzheimer's disease (AD) is the most common type of dementia. AD is pathologically characterized by synaptic dysfunction and cognitive decline due to the aggregation of a large amount of amyloid- $\beta$  (A $\beta$ ) protein in the brain. However, recent studies have discovered that the A $\beta$  is produced as an antimicrobial peptide that acts against bacteria and viruses. This has renewed interest in the effect of A $\beta$  on AD. Thus, in this study, we investigated the different concentrations of A $\beta$ 25–35 on neuroprotection and further explore the related mechanisms. Firstly, we detected the cognitive function using the Y-maze test, novel object recognition memory task and Morris water maze test. Then, we analyzed the ultrastructure of synapses and mitochondria, in addition to evaluating SOD levels. We also examined the effect of A $\beta$ 25–35 on the viability and structure of the primary neurons. The western blot analysis was used to measure the protein levels. The results showed that mice treated with high concentration of A $\beta$ 25–35 impaired the learning-memory ability and disordered the structure of neurons and mitochondria. Meanwhile, high concentration of A $\beta$ 25–35 decreased the SIRT1/Nrf2 related antioxidant capacity and induced apoptosis. In contrast, mice treated with low concentration of A $\beta$ 25–35 increased SOD levels and SIRT1/Nrf2 expressions, and induced autophagy. Our data suggest that low concentration of A $\beta$ 25–35 may increase SOD levels through SIRT1/Nrf2 and induce autophagy.

#### 1. Introduction

Alzheimer's disease (AD), one of the most deleterious neurodegenerative diseases, was initially described by Alois Alzheimer in 1906. The hypothesis stating amyloid and tau protein as the possible cause of AD is popular and widely accepted theory. However, an increasing number of studies have discovered that microorganisms exist in the brains of AD patients, confirming the correlation between microorganisms and AD (Fulop et al., 2018; Dominy et al., 2019). Hence, the infection hypothesis of AD has been proposed. Pathogens act as triggers to initiate amyloid  $\beta$  (A $\beta$ ) accumulation and formation of amyloid plaques, tau hyperphosphorylation, and inflammation in the brain of AD (Harris and Harris, 2015; Kumar et al., 2016; Dominy et al., 2019). A $\beta$ , normally produced by neurons is found in the brain throughout life during

synaptic activity to fulfill the physiological roles in maintaining synaptic plasticity and learning-memory mainly via activating of PI3K pathway and IGF-1 receptors, as well as maintaining antimicrobial protection via reducing microbial adhesion to host cells and entrapment of microbes (Giuffrida et al., 2009; Bourgade et al., 2016b; Kumar et al., 2016). While, pathological conditions such as infections, metabolic defects, misfolded proteins and other insults would increase A $\beta$  production to damage synapses and learning-memory which is related to inhibiting T-Type calcium channels mediated by Nogo receptor, inducing microglia activation and releasing of proinflammatory cytokines (Kumar et al., 2016; Zhao et al., 2017). Herein, we investigate the different concentrations of A $\beta_{25-35}$  in regulating neuroprotection.

Silent information regulator 1 (SIRT1), an NAD+-dependent protein deacetylase, is known to play an essential role in improving

E-mail address: pingmu@symc.edu.cn (P. Mu).

<sup>\*</sup> Corresponding author at: Department of Biochemistry and Molecular Biology, Shenyang Medical College, 146 Huanghe North Street, Yuhong District, Shenyang, Liaoning, 110034, People's Republic of China.

neurodegenerative diseases by influencing neuronal survival, synaptic plasticity, and cognitive function (Zhang et al., 2020). SIRT1 is highly expressed in the neurons of the brain, which is closely related to learning and memory. Overexpression of SIRT1 promotes neurite outgrowth and cell survival in neurons (Guo et al., 2011). Studies have shown that the expression of SIRT1 is reduced both in the patients and mice models for AD (Lutz et al., 2014; Corpas et al., 2017). Studies have shown that SIRT1 has been proposed to induce protective effects against AD pathology via multiple pathways, such as inhibiting tau hyperphosphorylation and regulating the synaptic plasticity of neurons (Michan et al., 2010; Min et al., 2010). Mitochondrial dysfunction greatly contributes to synaptic deficits and memory loss in the early phase of AD. The activation of SIRT1 can regulate nuclear factor E2 related factor 2 (Nrf2), which activates the transcription of genes encoding antioxidant enzymes (SOD, NQO-1, HO-1) and attenuates the Aβ-induced damage (Gong et al., 2017; Ma et al., 2018). Mitochondria are important organelles that play a central role in energy metabolism and apoptosis. Damaged mitochondria cause cytochrome c release into the cytoplasm and activate caspase 9, which ultimately induces cell apoptosis (Shin et al., 2018). Autophagy is essential for neuronal homeostasis that breaks down organelles and macromolecules. Autophagy is the process of eliminating microorganisms in the brain (Harris and Harris, 2015; Fang et al., 2019). Nrf2, as part of a protective response against oxidative damage of mitochondria, inhibits apoptosis and mediates autophagy (Pajares et al., 2016; Frias et al., 2020).

Aβ, a potent modulator, induces protein expression to regulate neuronal survival/death in neurodegenerative pathophysiology. Mice injected with Aβ<sub>25-35</sub> (9 nmol) induce neuronal death and cognition impaired through apoptosis (Zhi et al., 2014). However, incubation with  $A\beta_{40},$  the most common  $A\beta$  isotype, protects neurons at concentrations as low as 10 pM (Plant et al., 2003). Research also shows that  $A\beta_{42}$ (200 pM) enhances LTP and hippocampal-dependent memory by acting on  $\alpha 7$ -containing nicotinic acetylcholine receptors. In contrast, high concentration of  $A\beta_{42}$  (200 nM) impairs LTP (Puzzo et al., 2008). It is speculated that the opposite effects on learning-memory may be related to different concentrations of  $A\beta$ , and the possible mechanisms involved need to be studied. Herein, we investigated the potential roles of different concentrations of  $A\beta_{25-35}$  in neurons by measuring the SIRT1/Nrf2 modulated antioxidant capacity on autophagy and apoptosis in vivo and in vitro studies. Our study provides valuable insight into the role of  $A\beta$  production in the development of AD.

#### 2. Materials and methods

#### 2.1. Amyloid $\beta$ (25–35) preparation

The  $A\beta_{25-35}$  peptide (Sigma Aldrich, A4559) was dissolved in saline and incubated at 37 °C for 5 days to induce of  $A\beta_{25-35}$  aggregation (Zhu et al., 2018b).

#### 2.2. Animals and experimental schedule

Male Kunming (KM) mice (weighing 20–25 g, n = 23, 7–8 mice per group) were purchased from Liaoning Changsheng Biotechnology Co., Ltd. The mice were divided into three groups: Sham group, low concentration of  $A\beta_{25-35}$  group, and high concentration of  $A\beta_{25-35}$  group. Mice were housed under controlled conditions of temperature  $23\pm2\,^{\circ}\text{C}$ , humidity 50–60 %, and 12h light/dark cycle. Water and food were provided ad libitum. All animal procedures were approved by the Experimental Animal Ethics Committee of the Shenyang Medical College of China (SYYXY2019050801) and were implemented following the Guide for the Care and Use of Laboratory Animals. Mice in the low and high concentrations of  $A\beta_{25-35}$  groups received a unilateral and single intracerebroventricular injection (i.c.v.) of  $A\beta_{25-35}$  2 nmol/mouse or 9 nmol/mouse, respectively, using a Hamilton microsyringe, 3.0 mm dorsoventral (DV), 0.5 mm anteroposterior (AP), and 1.1 mm

mediolateral (ML) to the bregma. Mice in the sham group were injected with a vehicle (0.9 % NaCl). Behavioral tests using the double-blind method were started from day 5 to day 13 after  $A\beta_{25-35}$  injection, including novel object recognition memory task (days 5–6), Y-maze test (day 7) and Morris water maze (days 8–12, training session; day 13, probe trial). After the behavioral test, the mice were sacrificed on day 14 to further analysis. The experimental schedule is shown in Fig. 1.

During the surgical procedure, mice were anesthetized with an intraperitoneal injection of sodium pentobarbital (50 mg/kg) to minimize suffering. We initially used 8 mice in each group. One mouse in the low concentration of  $A\beta_{25-35}$  group did not wake up during the operation. The remaining animals (n = 7–8/group) were all tested behaviors. Four mice of each group were used for SOD assay and western blot (the left side of neocortex for SOD assay, and the other side for western blot). Three mice of each group were used for electron microscopy. One mouse left in sham or high concentration of  $A\beta_{25-35}$  group was not used in any experiment, except for behavioral tests.

#### 2.3. Novel object recognition memory task

The equipment consisted of a square box (length, 40 cm; height, 35 cm; width, 40 cm), and the test was performed as described previously (Zhu et al., 2018b). Before the test, the mice were habituated to the equipment for 10 min twice per day to minimize their fear of the unfamiliar environment. During the tests, two identical objects, A1 and A2, were placed at the center of the box. Mice were allowed to explore freely for 5 min. After a 1 h inter-trial interval, the familiar object A2 was replaced with a novel object B, and the mouse was permitted to explore the objects for another 5 min in a retention trial. Exploratory behavior was defined as directing the nose to the object at a distance of less than 2 cm or touching the object with the nose. The exploration time (s) for each object in each session was recorded. The discrimination index (DI) was calculated as follows: (time spent exploring object B or A2 - A1)/total exploration time.

#### 2.4. Y-maze test

The Y-maze test was used to detect working memory (Zhu et al., 2018a). The equipment comprised three brown wooden arms of the same size (length, 40 cm; height, 12 cm; width, 10 cm). Each mouse was allowed to explore freely in the maze for 5 min, and the entry sequence was recorded. One successful alternation was defined as the mouse entering into three arms consecutively. Alternation behavior was calculated as follows:

Alternation behavior = number of successful alternations/ (total number of entries - 2)  $\times 100$  %.

#### 2.5. Morris water maze test

The Morris water maze (MWM) test was performed from day 8 to day 13 after  $A\beta_{25-35}$  injection to assess spatial learning-memory function (long-term memory) (Zhu et al., 2018b). The MWM equipment (JiLiang, ShangHai) consisted of a round and black tank filled with water. During the training session (days 8–12), a black platform with a diameter of 10 cm was hidden 1 cm below the surface of the water in the middle of one quadrant. Mice were allowed to find the underwater platform within 60 s twice per day for continuous 5 days and the time was recorded as the escape latency. We calculated the escape latency between each group every day. Until the 5th day of training session, a significant difference of escape latency was observed between the  $A\beta_{25-35}$  (9 nmol) group and the sham group (Fig. 3a, P<0.05). During the probe trial session (day 13), the platform was removed from the pool. The swimming path and related data (time spent in the target quadrant, number of

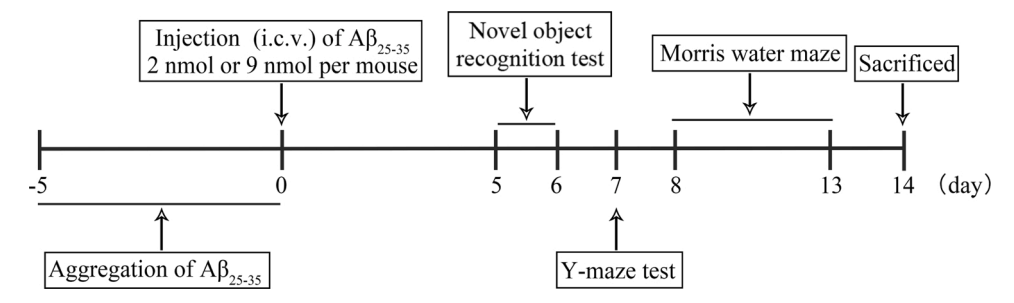


Fig. 1. Experimental schedule.

crossings of the former platform position, and swimming speed) were recorded for 60 s.

#### 2.6. Electron microscopy

The hippocampal and cortical samples were cut into small pieces  $(0.8-1.0~\mathrm{mm}^3)$  and fixed in 2.5 % glutaraldehyde in PBS at 4 °C overnight. Then, these samples were treated with 1 % osmium tetroxide at 4 °C for 3 h, dehydrated with graded ethanol and acetone, and embedded in resin. A 50 nm–thick section was cut and stained with 4 % uranyl acetate and 0.5 % ad citrate. The ultrastructure was observed using a transmission electron microscope (JEOL H-7650, Japan).

#### 2.7. Measurement of SOD activity

The homogenates of mice cerebral cortices were collected for immediate measurements of superoxide dismutase (SOD) using assay kits according to the manufacturer's instructions (S0101, Beyotime, China).

#### 2.8. Preparation and treatment of primary neurons

Primary neurons of cerebral cortices were obtained from mice born within 24 h (10–14 mice/litter). The cells were seeded into 96- or 6-well plates (1.0  $\times$   $10^6$  cells/mL) and cultured in a neurobasal medium supplemented with 2 % B27 following published protocols (Theurey et al., 2019). Primary neurons were treated with aggregated  $A\beta_{25-35}$  (2  $\mu M$  or 20  $\mu M$ ) after culturing for 5 days. After treatment with  $A\beta_{25-35}$  for 24 h, neuronal morphology, viability and protein levels were detected.

#### 2.9. Cell viability analysis

Cell viability was determined using the Cell Counting Kit-8 (CCK-8) reagent (Vazyne Biotech). Briefly, primary cortical neurons were plated into 96-well plates. After being treated with  $A\beta_{25-35}$  for 24 h, 10  $\mu L$  of CCK8 reagent and 90  $\mu L$  of the medium were added into each well and incubated for another 2 h at 37 °C. The absorbance at 450 nm was measured by using a microplate reader (CLARIOstar, BMG LABTECH, Germany).

#### 2.10. Western blot analysis

The samples were extracted using lysis buffer with 1 % PMSF and quantified using a BCA assay kit (Zhang et al., 2020). Protein samples (20–50 µg) were separated on 8–12 % SDS-PAGE and transferred to PVDF membranes. Then the following primary antibodies were used: Postsynaptic density protein (PSD95, 1:1000, 36233, CST), Synapsin 1 (SYN-1, 1:1200, 5297, CST), NeuN (1:1000, 24307, CST), SIRT1 (1:1000, ab110304, Abcam), Nrf2 (1:1000, ab31163, Abcam), LC3 (1:1000, PM036, MBL), Bax (1:4000, 50599–2-AP, Proteintech), Bcl2 (1:1000, 12789–1-AP, Proteintech), Cleaved-Caspase3 (1:800, ab32042, Abcam),  $\beta$ -actin (1:400, sc-47778, Santa Cruz), and secondary antibodies (1:8000, Absin, abs20040ss and abs20039ss). Primary antibodies were incubated overnight at 4 °C and protein bands were

visualized using an ECL kit. Immunoblotting images were obtained by using an automatic chemiluminescence image analysis system (Tanon, 5500, PRC), and analyzed by using the Image J software version 1.37. The samples were normalized to  $\beta$ -actin.

#### 2.11. Statistical analyses

The qualitative data are representative of at least three trials. Quantitative data are expressed as mean  $\pm$  SD. Statistical analysis was conducted using the SPSS 26. Statistical differences in multiple groups were determined by the one-way analysis of variance (ANOVA) followed by the LSD multiple comparisons test with homogeneity or Dunnett's T3 test with heterogeneity of variance. A value of P < 0.05 was considered to be statistically significant.

#### 3. Results

### 3.1. Different concentrations of $A\beta_{25-35}$ mediates the cognitive ability in KM mice

Further, we investigated the effects of different concentrations of  $A\beta_{25-35}$  on the regulation of cognitive ability. The novel object recognition test and Y-maze test, revealing imaginal memory and working memory, respectively, were performed in Aβ<sub>25-35</sub>-injected mice to evaluate short-term memory. Injection of  $A\beta_{25-35}$  (9 nmol) into the lateral ventricle of mice decreased the discrimination index (P < 0.05) and alternation behavior (P < 0.001) compared to that of the sham group, indicating that high concentration of  $A\beta_{25-35}$  (9 nmol) injection impaired imaginal memory (Fig. 2 a) and working memory (Fig. 2 b,c). However, no significant differences were observed between the low concentration of  $A\beta_{25-35}$  (2 nmol) and sham groups (Fig. 2). The Morris water maze was performed in mice to evaluate spatial memory as longterm memory. Compared to the sham group, mice in the  $A\beta_{25-35}$ (9 nmol) group showed increased escape latency during the training period (Fig. 3a, P < 0.05), while decreasing the number of crossings of the platform (P < 0.01) and spent more time (P < 0.05) in the target quadrant after the platform was removed (Table 1). However, there were no significant differences between the  $A\beta_{25-35}$  (2 nmol) group and the sham group (Fig. 3 and Table1). These results indicated that mice injected with high concentration of  $A\beta_{25-35}$  (9 nmol) impaired cognitive memory, but the low concentration of  $A\beta_{25-35}$  (2 nmol) could not do so.

#### 3.2. Different roles of $A\beta_{25-35}$ in neurons and mitochondria in KM mice

Aβ has a potential protective role as an antimicrobial peptide. To evaluate the different concentrations of  $Aβ_{25-35}$  in the synapses and mitochondria, the ultrastructure morphology was observed using a transmission electron microscope. Mice in the  $Aβ_{25-35}$  (9 nmol) group showed an ambiguous synaptic structure with fused presynaptic and postsynaptic membrane and disappeared synaptic gap, and impaired mitochondria with collapsed cristae (Fig. 4a), meanwhile decreased synaptic related protein expression of PSD95, SYN-1, NeuN (Fig. 4c–f, P < 0.001), and SOD levels (Fig. 4b, P < 0.01) compared with the sham

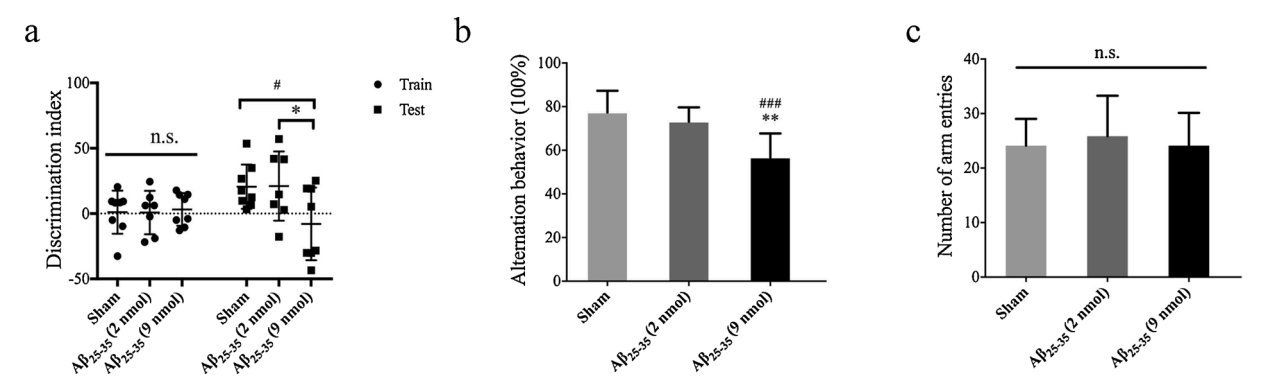


Fig. 2. Effect of  $Aβ_{25-35}$  on short-term memory impairment of KM mice. (a) Visual recognition in the novel object recognition test. (b) Spontaneous alternation behavior and (c) total number of arm entries in the Y-maze test. The data represented as mean  $\pm$  SD, n = 7-8.  $^{\#}P < 0.05$ ,  $^{\#\#}P < 0.001$  versus Sham;  $^{*}P < 0.05$ ,  $^{**}P < 0.01$  versus  $Aβ_{25-35}$  (2 nmol).

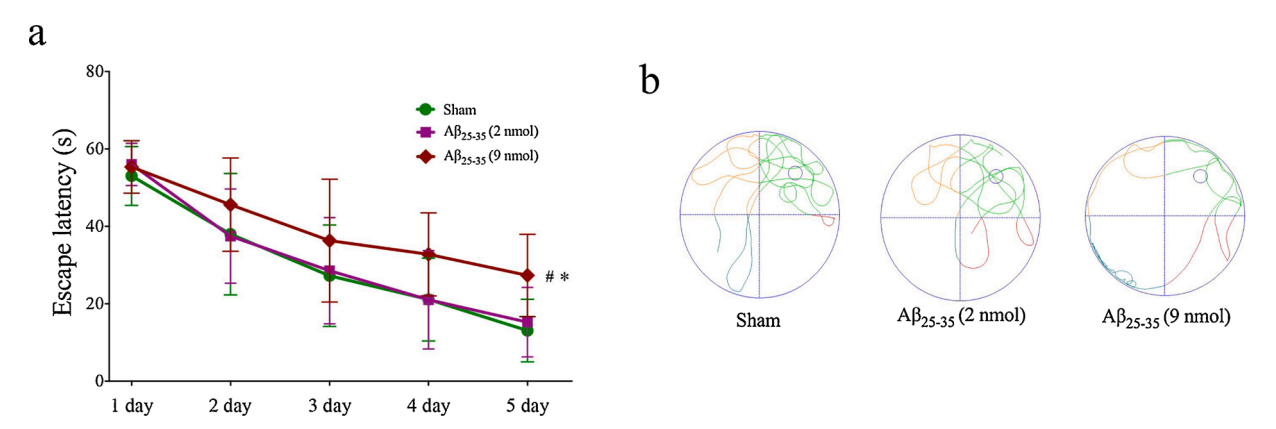


Fig. 3. Effect of  $A\beta_{25-35}$  on long-term memory impairment of KM mice. (a) The escape latency during 5 days of the Morris Water Maze test. (b) The representative track map of each group of mice. The data represented as mean  $\pm$  SD, n = 7-8.  $^{\#}P < 0.05$  versus Sham;  $^{*}P < 0.05$  versus  $A\beta_{25-35}$  (2 nmol).

Table 1 Different concentrations of A $\beta_{25-35}$  on spatial memory in mice.

Group	Grossing the platform (NO.)	Time of target quadrant (s)	Average speed (mm/s)
Sham	$2.50 \pm 1.20$	25.79 ± 5.44	207.80 ± 52.04
Αβ <sub>25–35</sub> (2 nmol)	$2.00\pm1.00$	$25.58 \pm 7.06$	$189.61 \pm 28.23$
Αβ <sub>25–35</sub> (9 nmol)	$0.63 \pm 0.52^{\#\#}$ *	$17.51 \pm 6.34$ *	$192.53 \pm 45.15$

All the results are expressed as mean  $\pm$  SD, n = 7–8.  $^{\#}P$  < 0.05,  $^{\#\#}P$  < 0.01 versus Sham;  $^{*}P$  < 0.05 versus A $\beta_{25-35}$  (2 nmol).

group. Mice in the A $\beta_{25-35}$  (2 nmol) group showed a clear synaptic structure and mitochondrial cristae (Fig. 4a) and maintained the synaptic-related proteins at normal levels (Fig. 4c–f). However, the most relevant finding in our study is that mice injected with A $\beta_{25-35}$  (2 nmol) showed increased SOD levels compared to the sham group (Fig. 4b, P < 0.05). This suggests that low concentration of A $\beta_{25-35}$  might produce an antioxidant response.

## 3.3. Different roles of $A\beta_{25-35}$ in SIRT1/Nrf2 regulated apoptosis and autophagy in KM mice

We further determined the expression of the mitochondrion-related proteins, including SIRT1 and Nrf2. Western blot analysis showed that protein expression of SIRT1 (P < 0.01) and Nrf2 (P < 0.01) in the A $\beta_{25-35}$  (9 nmol) group were both decreased, whereas in the A $\beta_{25-35}$  (2 nmol) group (SIRT1, P < 0.05; Nrf2, P < 0.05) were significantly increased compared with those in the sham group (Fig. 5a–c). We then tested

whether low concentration of  $A\beta_{25-35}$  regulated SIRT1/Nrf2 related to apoptosis and autophagy in mice. The results showed the increased expression of Bax (P < 0.01), Bax/Bcl2 (P < 0.01), and Cleaved-Caspase3 (P < 0.001), and decreased expression of Bcl2 (P < 0.05), LC3 (P < 0.01), and LC3 II/I (P < 0.01) in the  $A\beta_{25-35}$  (9 nmol) group compared with the sham group (Fig. 5d–i). However, mice in the  $A\beta_{25-35}$  (2 nmol) group showed no significance in apoptosis-related proteins (Fig. 5d–g), but an increased expression of LC3II/I (Fig. 5i, P < 0.05). This demonstrated that low concentration of  $A\beta_{25-35}$  induced SIRT1/Nrf2 related to autophagy, but not apoptosis.

#### 3.4. Different concentrations of $A\beta_{25-35}$ in primary neurons

To further test the effect of different concentrations of  $A\beta_{25-35}$ , the primary cultures of cortices were used in the study of mice born within 24 h. It showed that high concentration of  $A\beta_{25-35}$  (20  $\mu$ M) produced neuronal death as measured by CCK8 (Fig. 6a, P < 0.05), and impaired neuronal morphology (shorten the length of dendrites and reduce the complexity of the branches) (Fig. 6b). Western blot analysis revealed that primary neurons treated with  $A\beta_{25-35}$  (20  $\mu$ M) decreased the protein expression of neuronal structure associated proteins, including PSD95, SYN-1, and NeuN, compared with the control group (Fig. 6c-f, P < 0.01). However, low concentration of  $A\beta_{25-35}$  (2  $\mu$ M) did not affect these *in vitro* study (Fig. 6).

### 3.5. Different roles of $A\beta_{25-35}$ in apoptosis and autophagy in primary neurons

Subsequently, the protein levels of different concentrations of

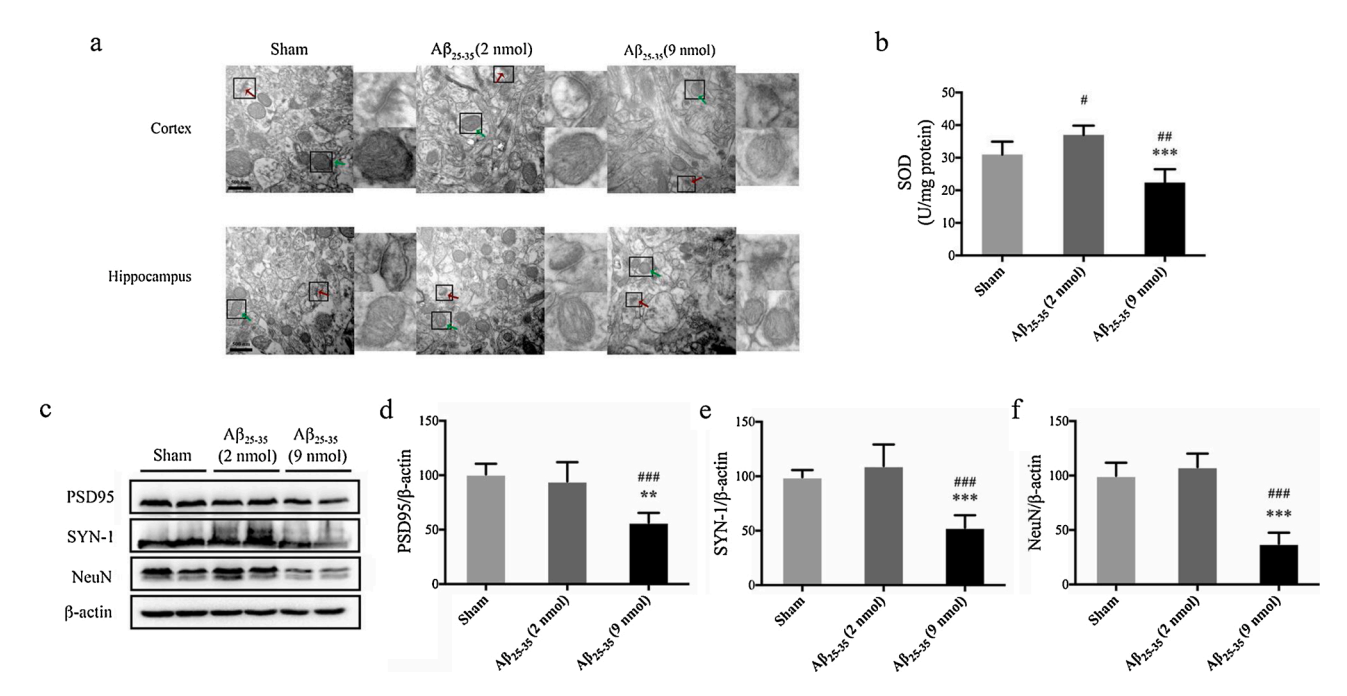
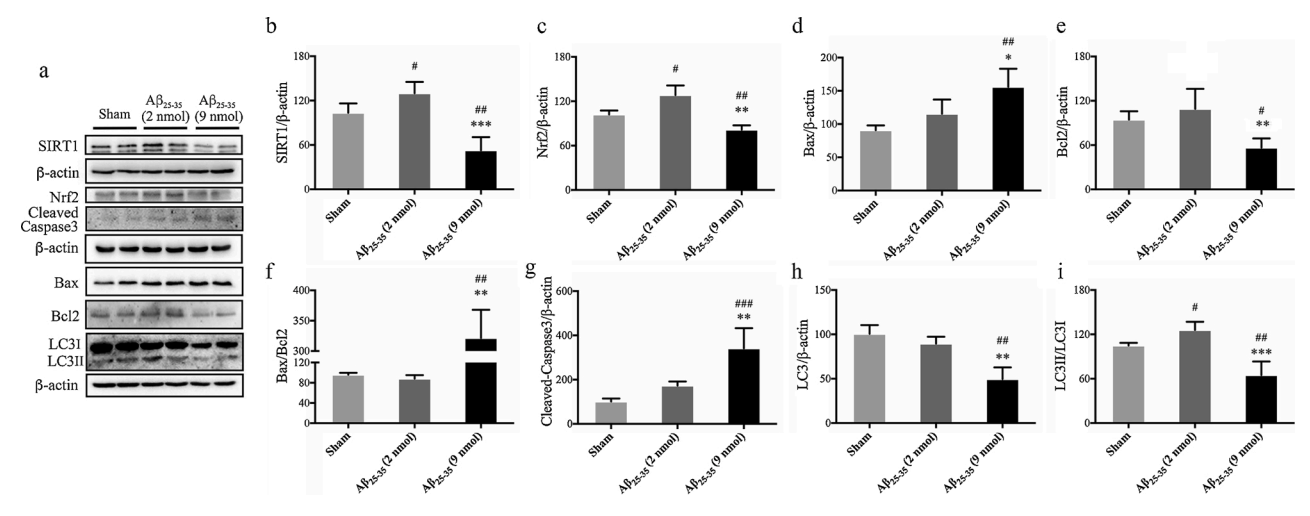


Fig. 4. Effect of  $A\beta_{25-35}$  on the neuronal and mitochondrial structure in the brain of mice. (a) Transmission electron microscopy images of synaptic and mitochondrial structure in each group. Red indicates synapses and green indicates mitochondria. n=3. (b) Antioxidant enzyme activity of SOD was measured in the cortex of mice. (c) Western blot bands and (d–f) densitometric quantification of PSD95, SYN-1, and NeuN in the cortex of mice. The data represented as mean  $\pm$  SD, n=4.  $^{\#}P<0.05$ ,  $^{\#\#}P<0.01$ ,  $^{\#\#}P<0.001$  versus Sham;  $^{**}P<0.01$ ,  $^{**}P<0.01$  versus  $A\beta_{25-35}$  (2 nmol).



**Fig. 5.** Effect of Aβ<sub>25-35</sub> on SIRT1-associated apoptosis and autophagy in the cortex of mice. (a) Representative western blot bands of SIRT1, Nrf2, Cleaved-Caspase3, Bax, Bcl2, and LC3 in the cerebral cortex of mice. (b–c) Densitometric quantification of SIRT1 and Nrf2 expression. (d–g) Densitometric quantification of apoptosis-associated protein expression. (h–i) Densitometric quantification of autophagy-associated protein expression. The data represented as mean  $\pm$  SD, n = 4.  $^\#P$  < 0.05,  $^{\#P}$  < 0.01,  $^{\#\#P}$  < 0.001 versus Sham;  $^*P$  < 0.05,  $^{**P}$  < 0.01,  $^{***P}$  < 0.001 versus Aβ<sub>25-35</sub> (2 nmol).

Aβ<sub>25–35</sub> in SIRT1/Nrf2 related proteins were evaluated in the primary neurons. Western blot analysis is shown in Fig. 7a, and quantitative analysis revealed that neurons treated with Aβ<sub>25–35</sub> (20 μM) decreased the protein expression of SIRT1 (P < 0.01) and Nrf2 (P < 0.05), and increased the protein expression of Bax (P < 0.01) (Fig. 7a–d). Neuronal treatment with Aβ<sub>25–35</sub> (2 μM) increased the protein expression of SIRT1 (P < 0.05) and LC3 (P < 0.01) (Fig. 7b, e), and had an increasing trend in the protein expression of Nrf2 (Fig. 7c).

#### 4. Discussion/Conclusion

AD is an age-related neurodegenerative disease with two main pathological features in the brain-the presence of extracellular senile plaques composed of A $\beta$  protein, and intracellular neurofibrillary tangles composed of p-Tau protein (Kikuchi et al., 2017). In recent years, research has shown that AD is related to the microorganisms that invade the brain. Infection with microorganisms can cause the accumulation of A $\beta$ , gradually forming plaques, which are gathered together to fight bacteria to produce a protective response in the brain (Kumar et al., 2016; Dominy et al., 2019). A $\beta$  is derived from the sequential cleavage of amyloid- $\beta$  precursor protein by the  $\beta$ - and  $\gamma$ -secretase enzymes (Vassar et al., 1999). However, the overproduction of A $\beta$  in the brain is neurotoxic, which can lead to neuronal synapse dysfunction, tau hyperphosphorylation, and cognitive decline (Rottkamp et al., 2001). A $\beta$ 25-35 is often used as a convenient alternative model drug in AD investigations, which has a smaller 11-amino acid fragment of the

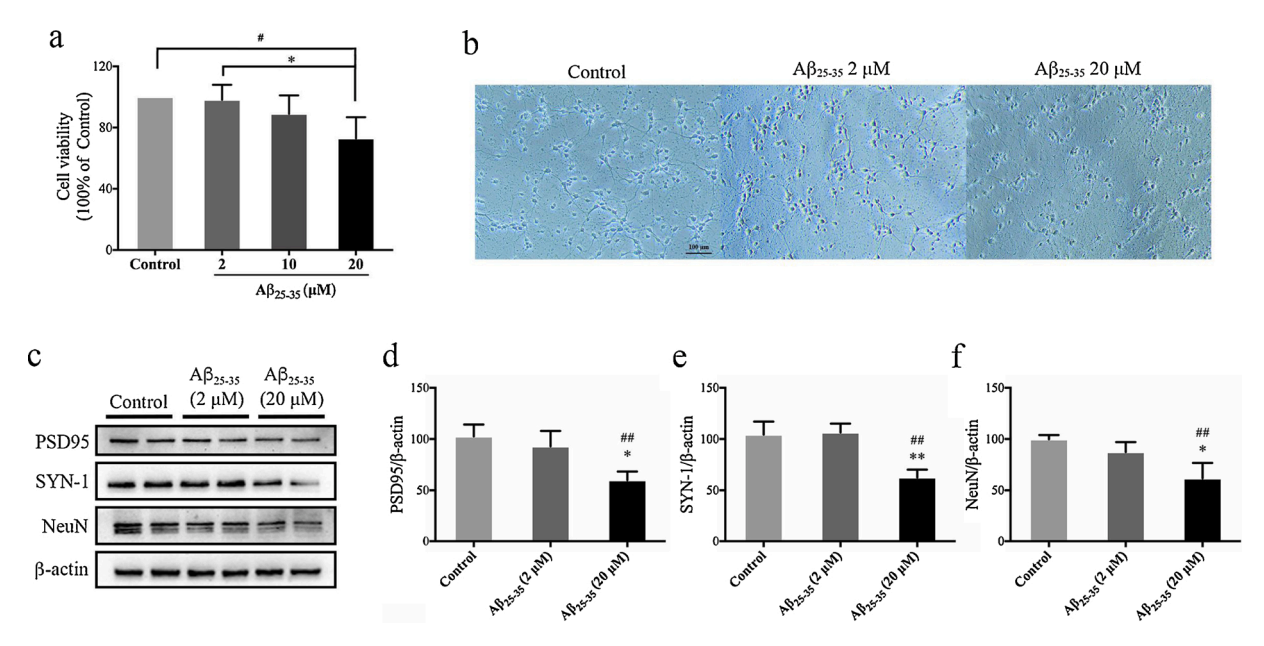


Fig. 6. Effect of  $Aβ_{25-35}$  on the primary neurons. (a) The viability and (b) morphological structure of primary neurons treated with  $Aβ_{25-35}$ . (c) Western blot bands and (d–f) densitometric quantification of PSD95, SYN-1, and NeuN in the primary neurons. The data represented as mean  $\pm$  SD, n = 3.  $^\#P < 0.05$ ,  $^\#P < 0.01$  versus Control;  $^*P < 0.05$ ,  $^*P < 0.01$  versus  $Aβ_{25-35}$  (2 μM).

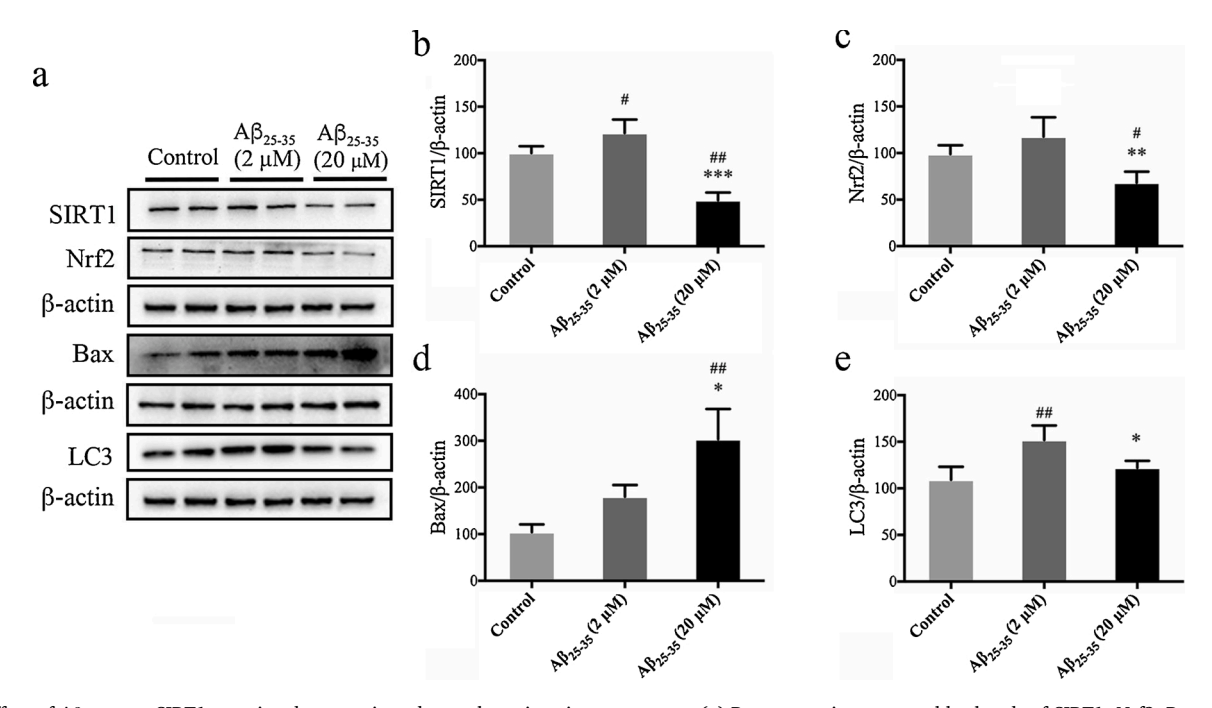


Fig. 7. Effect of  $A\beta_{25-35}$  on SIRT1-associated apoptosis and autophagy in primary neurons. (a) Representative western blot bands of SIRT1, Nrf2, Bax, and LC3 in primary neurons. (b–c) Densitometric quantification of SIRT1 and Nrf2 expression. (d–e) Densitometric quantification of Bax and LC3 expression. The data represented as mean  $\pm$  SD, n = 3.  $^\#P < 0.05$ ,  $^{\#\#P} < 0.01$  versus Control;  $^*P < 0.05$ ,  $^{**P} < 0.01$ ,  $^{**P} < 0.01$  versus  $A\beta_{25-35}$  (2  $\mu$ M).

full-length peptide and can retain most of the toxicological properties of  $A\beta_{1-40}$  and  $A\beta_{1-42}$  (Varadarajan et al., 2001). Therefore, it is necessary to explore the effect of  $A\beta_{25-35}$  on neuroprotection. According to the literature, different concentrations of  $A\beta_{42}$  have the opposite effects on neuronal function and learning-memory (Puzzo et al., 2008). Herein, we investigate whether different concentrations of  $A\beta_{25-35}$  have different effects on learning-memory and the possible mechanisms involved.

Maintaining the stability of synapses and mitochondria is closely related to learning-memory ability (da Silva et al., 2020; Kumar and Reddy, 2020). Learning-memory ability can be tested by animal behavior (Zhi et al., 2014). Pathological changes in AD can damage

animal behavior and learning-memory (Lok et al., 2013). In this study, animal behaviors including the novel object recognition, Y-maze test, and MWM were used to assess learning-memory performance. In the behavioral experiments, we firstly carried out the less irritating experiments (novel object recognition and Y-maze test), and then MWM was conducted in order to reduce the environmental irritation to animals. Our results showed that mice treated with high concentration of  $A\beta_{25-35}$  impaired imaginal memory, working memory, and spatial memory. Meanwhile, mice in high concentration of  $A\beta_{25-35}$  group showed an ambiguous synaptic structure and decreased the expression of PSD95, SYN-1, and NeuN. In contrast, the low concentration of  $A\beta_{25-35}$  group

showed a clear synaptic structure, including presynaptic membrane, synaptic cleft, and postsynaptic membrane, and normal levels of PSD95, SYN-1, and NeuN. This suggested that treatment with high concentration of Aβ<sub>25-35</sub> impaired neurons and learning-memory ability, while low concentration did not. Previous studies have shown that mitochondria are widely distributed in axons, dendrites, and presynaptic terminals, which is crucial for cognitive function (Cheng et al., 2010; Hebert-Chatelain et al., 2016). Mitochondrial dysfunction plays an important role in neurodegenerative diseases. One of the reasons for the neurotoxicity of  $A\beta_{25-35}$  is to induce apoptosis via the mitochondrial pathway and increase the production of ROS (Gao et al., 2020). Both AD model mice and Aβ-treated neurons show the impaired mitochondria and decreased SOD levels (Cao et al., 2018; Liu et al., 2021). In our study, incomplete mitochondrial ridges and decreased SOD levels were found in mice of high concentration of  $A\beta_{25-35}$  group compared with sham group. However, the low concentration of the  $A\beta_{25-35}$  group in our study showed a clear structure of mitochondrial cristae and the increased SOD levels. These results indicated that treatment with high concentration of  $A\beta_{25-35}$  impaired the structure of mitochondria and decreased SOD levels, however low concentration of A<sub>β25-35</sub> did not damage neurons and mitochondria, but increased SOD levels.

Nrf2, a key redox-regulated gene, plays a critical role in alleviating oxidative stress by increasing SOD levels (Murphy et al., 2018; Bahn et al., 2019). A previous study showed that increased SIRT1 promotes the activation of Nrf2, resulting in the upregulation of Nrf2-related antioxidant capacity (da Cunha and Arruda, 2017). Therefore, we considered that the change in SOD levels might be related to SIRT1/Nrf2. In our study, the expression of SIRT1 and Nrf2 were both decreased at high concentration of Aβ<sub>25-35</sub> group compared with sham group. Interestingly, low concentration of  $A\beta_{25-35}$  tended to increase the expression of SIRT1/Nrf2. These results suggested that different concentrations of  $A\beta_{25-35}$  had the opposite effect on the antioxidant capacity induced by SIRT1/Nrf2. In the current study, accumulating evidence has shown that SIRT1/Nrf2 regulating antioxidant capacity influences apoptosis and autophagy in the cells (Guo et al., 2011; Liu et al., 2018; Yen et al., 2017; Lu et al., 2020). Meanwhile, SIRT1 can inhibit apoptosis (Zheng and Lu, 2016) and regulate autophagy-related genes (Atgs) by activating the FOXO to induce autophagy (Duan et al., 2016; Zhang et al., 2016), which protects cells against oxidative stress. Our results showed that high concentration of  $A\beta_{25\text{--}35}$  impaired apoptosis and autophagy in the neurons compared with sham (control) group. In contrast, the low concentration of  $A\beta_{25-35}$  showed no effect on apoptosis but promoted autophagy. These results suggested that high concentration of  $A\beta_{25-35}$  caused oxidative damage to impair apoptosis and autophagy through decreasing the expression of SIRT1/Nrf2. Whereas low concentration of A\(\beta\_{25-35}\) could produce antioxidant capacity through increasing the expression of SIRT1/Nrf2 and induce autophagy. It is speculated that upregulation of SIRT1 may be used to resist the neuronal damage caused by high concentration of  $A\beta_{25-35}$ .

In summary, different concentrations of  $A\beta_{25-35}$  have different roles in learning-memory. High concentration of  $A\beta_{25-35}$  impaired neurons and mitochondria, decreased SIRT1/Nrf2 related antioxidant capacity and dysregulated apoptosis and autophagy. However, low concentration of  $A\beta_{25-35}$  did not cause any damage to neurons and mitochondria, but increased SOD levels possibly through increasing SIRT1/Nrf2 and induced autophagy.

Herein, we support the studies that have proposed (Bourgade et al., 2016a; Kumar et al., 2016) that the production of  $A\beta$  might be beneficial for cells at first, but chronic accumulation might gradually become harmful.

#### Author statement

We declare that this manuscript entitled "Amyloid- $\beta$  (25–35) regulates neuronal damage and memory loss via SIRT1/Nrf2 in the cortex of mice" is original, has not been published before and is not currently

being considered for publication elsewhere.

We confirm that the manuscript has been read and approved by all named authors (Zhu Lin, Lu Fangjin, Jia Xiaoyu, Yan Qiuying, Zhang Xiaoran and Mu Ping) and that there are no other persons who satisfied the criteria for authorship but are not listed. We further confirm that the order of authors listed in the manuscript has been approved by all of us.

#### **Author contributions**

ZL designed the research and wrote the paper; MP funded the research; LFJ and JXY analyzed the data; YQY and ZXR performed the research. All authors have reviewed the manuscript.

#### Ethical statement

All animal procedures were approved by the Experimental Animal Ethics Committee of the Shenyang Medical College of China (SYYXY2019050801) and were implemented following the Guide for the Care and Use of Laboratory Animals.

#### **Funding sources**

This work was supported by the Natural Science Foundation of Liaoning Province (2019-ZD-0327 and 20180550491), the Xingliao Talent Project (XLYC1802055 and XLYC1807116), and the Science and Technology Fund of Shenyang Medical College (20186057 and 20191032).

#### **Declaration of Competing Interest**

The authors report no declarations of interest.

#### References

- Bahn, G., Park, J.-S., Yun, U.J., Lee, Y.J., Choi, Y., Park, J.S., Baek, S.H., Choi, B.Y., Cho, Y.S., Kim, H.K., Han, J., Sul, J.H., Baik, S.-H., Lim, J., Wakabayashi, N., Bae, S. H., Han, J.-W., Arumugam, T.V., Mattson, M.P., Jo, D.-G., 2019. NRF2/ARE pathway negatively regulates BACE1 expression and ameliorates cognitive deficits in mouse Alzheimer's models. Proc. Natl. Acad. Sci. 116 (25), 12516–12523. https://doi.org/10.1073/nnas.1819541116
- Bourgade, K., Dupuis, G., Frost, E.H., Fülöp, T., 2016a. Anti-viral properties of Amyloid-β peptides. J. Alzheimer Dis. 54 (3), 859–878. https://doi.org/10.3233/jad-160517.
   Bourgade, K., Le Page, A., Bocti, C., Witkowski, J.M., Dupuis, G., Frost, E.H., Fulop Jr, T., 2016b. Protective effect of amyloid-beta peptides against herpes simplex Virus-1 infection in a neuronal cell culture model. J. Alzheimers Dis. 50 (4), 1227–1241. https://doi.org/10.3233/jad-150652.
- Cao, K., Dong, Y.T., Xiang, J., Xu, Y., Hong, W., Song, H., Guan, Z.Z., 2018. Reduced expression of SIRT1 and SOD-1 and the correlation between these levels in various regions of the brains of patients with Alzheimer's disease. J. Clin. Pathol. 71 (12), 1090–1099. https://doi.org/10.1136/jclinpath-2018-205320.
- Cheng, A., Hou, Y., Mattson, M.P., 2010. Mitochondria and neuroplasticity. ASN Neuro 2 (5), e00045. https://doi.org/10.1042/AN20100019.
- Corpas, R., Revilla, S., Ursulet, S., Castro-Freire, M., Kaliman, P., Petegnief, V., Gimenez-Llort, L., Sarkis, C., Pallas, M., Sanfeliu, C., 2017. SIRT1 overexpression in mouse Hippocampus Induces cognitive enhancement through proteostatic and neurotrophic mechanisms. Mol. Neurobiol. 54 (7), 5604–5619. https://doi.org/10.1007/s12035-016-0087-9
- da Cunha, M.S.B., Arruda, S.F., 2017. Tucum-do-Cerrado (Bactris setosa mart.) may promote anti-aging effect by upregulating SIRT1-Nrf2 pathway and attenuating oxidative stress and inflammation. Nutrients 9 (11), 1243. https://doi.org/10.3390/ nu9111243.
- da Silva, J.S., Nonose, Y., Rohden, F., Lukasewicz Ferreira, P.C., Fontella, F.U., Rocha, A., Brochier, A.W., Apel, R.V., de Lima, T.M., Seminotti, B., Amaral, A.U., Galina, A., Souza, D.O., 2020. Guanosine neuroprotection of presynaptic mitochondrial calcium homeostasis in a mouse study with amyloid-beta oligomers. Mol. Neurobiol. 57 (11), 4790–4809. https://doi.org/10.1007/s12035-020-02064-4.
- Dominy, S.S., Lynch, C., Ermini, F., Benedyk, M., Marczyk, A., Konradi, A., Nguyen, M., Haditsch, U., Raha, D., Griffin, C., Holsinger, L.J., Arastu-Kapur, S., Kaba, S., Lee, A., Ryder, M.I., Potempa, B., Mydel, P., Hellvard, A., Adamowicz, K., Hasturk, H., Walker, G.D., Reynolds, E.C., Faull, R.L.M., Curtis, M.A., Dragunow, M., Potempa, J., 2019. Porphyromonas gingivalisin Alzheimer's disease brains: evidence for disease causation and treatment with small-molecule inhibitors. Sci. Adv. 5 (1), eaau3333 https://doi.org/10.1126/sciadv.aau3333.
- Duan, W.-J., Li, Y.-F., Liu, F.-L., Deng, J., Wu, Y.-P., Yuan, W.-L., Tsoi, B., Chen, J.-L., Wang, Q., Cai, S.-H., Kurihara, H., He, R.-R., 2016. A SIRT3/AMPK/autophagy network orchestrates the protective effects of trans-resveratrol in stressed peritoneal

- macrophages and RAW 264.7 macrophages. Free Radic. Biol. Med. 95, 230–242. https://doi.org/10.1016/j.freeradbiomed.2016.03.022.
- Fang, E.F., Hou, Y., Palikaras, K., Adriaanse, B.A., Kerr, J.S., Yang, B., Lautrup, S., Hasan-Olive, M.M., Caponio, D., Dan, X., Rocktaschel, P., Croteau, D.L., Akbari, M., Greig, N.H., Fladby, T., Nilsen, H., Cader, M.Z., Mattson, M.P., Tavernarakis, N., Bohr, V.A., 2019. Mitophagy inhibits amyloid-beta and tau pathology and reverses cognitive deficits in models of Alzheimer's disease. Nat. Neurosci. 22 (3), 401–412. https://doi.org/10.1038/s41593-018-0332-9.
- Frias, D.P., Gomes, R.L.N., Yoshizaki, K., Carvalho-Oliveira, R., Matsuda, M., Junqueira, M.S., Teodoro, W.R., Vasconcellos, P.C., Pereira, D.C.A., Conceicao, P.R. D., Saldiva, P.H.N., Mauad, T., Macchione, M., 2020. Nrf2 positively regulates autophagy antioxidant response in human bronchial epithelial cells exposed to diesel exhaust particles. Sci. Rep. 10 (1), 3704. https://doi.org/10.1038/s41598-020-59930-3.
- Fulop, T., Witkowski, J.M., Bourgade, K., Khalil, A., Zerif, E., Larbi, A., Hirokawa, K., Pawelec, G., Bocti, C., Lacombe, G., Dupuis, G., Frost, E.H., 2018. Can an infection hypothesis explain the beta amyloid hypothesis of Alzheimer's disease? Front. Aging Neurosci. 10, 224. https://doi.org/10.3389/fnagi.2018.00224.
- Gao, L., Zhou, F., Wang, K.-x., Zhou, Y.-z., Du, G.-h., Qin, X.-m., 2020. Baicalein protects PC12 cells from Aβ25–35-induced cytotoxicity via inhibition of apoptosis and metabolic disorders. Life Sci. 248, 117471 https://doi.org/10.1016/j. lfs.2020.117471.
- Giuffrida, M.L., Caraci, F., Pignataro, B., Cataldo, S., De Bona, P., Bruno, V., Molinaro, G., Pappalardo, G., Messina, A., Palmigiano, A., Garozzo, D., Nicoletti, F., Rizzarelli, E., Copani, A., 2009. Beta-amyloid monomers are neuroprotective. J. Neurosci. 29 (34), 10582–10587. https://doi.org/10.1523/JNEUROSCI.1736-09.2009.
- Gong, W., Li, J., Chen, Z., Huang, J., Chen, Q., Cai, W., Liu, P., Huang, H., 2017.
  Polydatin promotes Nrf2-ARE anti-oxidative pathway through activating CKIP-1 to resist HG-induced up-regulation of FN and ICAM-1 in GMCs and diabetic mice kidneys. Free Radic. Biol. Med. 106, 393–405. https://doi.org/10.1016/j.freeradbiomed.2017.03.003.
- Guo, W., Qian, L., Zhang, J., Zhang, W., Morrison, A., Hayes, P., Wilson, S., Chen, T., Zhao, J., 2011. Sirt1 overexpression in neurons promotes neurite outgrowth and cell survival through inhibition of the mTOR signaling. J. Neurosci. Res. 89 (11), 1723–1736. https://doi.org/10.1002/jnr.22725.
- Harris, S.A., Harris, E.A., 2015. Herpes simplex virus type 1 and other pathogens are key causative factors in sporadic Alzheimer's disease. J. Alzheimers Dis. 48 (2), 319–353. https://doi.org/10.3233/JAD-142853.
- Hebert-Chatelain, E., Desprez, T., Serrat, R., Bellocchio, L., Soria-Gomez, E., Busquets-Garcia, A., Pagano Zottola, A.C., Delamarre, A., Cannich, A., Vincent, P., Varilh, M., Robin, L.M., Terral, G., García-Fernández, M.D., Colavita, M., Mazier, W., Drago, F., Puente, N., Reguero, L., Elezgarai, I., Dupuy, J.-W., Cota, D., Lopez-Rodriguez, M.-L., Barreda-Gómez, G., Massa, F., Grandes, P., Bénard, G., Marsicano, G., 2016. A cannabinoid link between mitochondria and memory. Nature 539 (7630), 555–559. https://doi.org/10.1038/nature20127.
- Kikuchi, K., Kidana, K., Tatebe, T., Tomita, T., 2017. Dysregulated metabolism of the amyloid-beta protein and therapeutic approaches in Alzheimer disease. J. Cell. Biochem. 118 (12), 4183–4190. https://doi.org/10.1002/jcb.26129.
- Kumar, S., Reddy, P.H., 2020. The role of synaptic microRNAs in Alzheimer's disease. Biochim. Biophys. Acta Mol. Basis Dis. 1866 (12), 165937 https://doi.org/10.1016/j.bbadis.2020.165937.
- Kumar, D.K.V., Choi, S.H., Washicosky, K.J., Eimer, W.A., Tucker, S., Ghofrani, J., Lefkowitz, A., McColl, G., Goldstein, L.E., Tanzi, R.E., Moir, R.D., 2016. Amyloid-β peptide protects against microbial infection in mouse and worm models of Alzheimer's disease. Sci. Transl. Med. 8, 340ra72 https://doi.org/10.1126/ scitzaslmed.aafi.059
- Liu, X., Ma, Y., Wei, X., Fan, T., 2018. Neuroprotective effect of licochalcone A against oxygen-glucose deprivation/reperfusion in rat primary cortical neurons by attenuating oxidative stress injury and inflammatory response via the SIRT1/Nrf2 pathway. J. Cell. Biochem. 119 (4), 3210–3219. https://doi.org/10.1002/jcb.26477.
- Liu, X., Chu, B., Jin, S., Li, M., Xu, Y., Yang, H., Feng, Z., Bi, J., Wang, P., 2021. Vascular endothelial growth factor alleviates mitochondrial dysfunction and suppression of mitochondrial biogenesis in models of Alzheimer's disease. Int. J. Neurosci. 131 (2), 154–162. https://doi.org/10.1080/00207454.2020.1733564.
- Lok, K., Zhao, H., Zhang, C., He, N., Shen, H., Wang, Z., Zhao, W., Yin, M., 2013. Effects of accelerated senescence on learning and memory, locomotion and anxiety-like behavior in APP/PS1 mouse model of Alzheimer's disease. J. Neurol. Sci. 335 (1-2), 145–154. https://doi.org/10.1016/j.jns.2013.09.018.
- Lu, J., Huang, Q., Zhang, D., Lan, T., Zhang, Y., Tang, X., Xu, P., Zhao, D., Cong, D., Zhao, D., Sun, L., Li, X., Wang, J., 2020. The protective effect of DiDang tang against AlCl3-Induced oxidative stress and apoptosis in PC12 cells through the activation of SIRT1-Mediated Akt/Nrf2/HO-1 pathway. Front. Pharmacol. 11, 466. https://doi.org/10.3389/fphar.2020.00466.
- Lutz, M.I., Milenkovic, I., Regelsberger, G., Kovacs, G.G., 2014. Distinct patterns of sirtuin expression during progression of Alzheimer's disease. Neuromolecular Med. 16 (2), 405–414. https://doi.org/10.1007/s12017-014-8288-8.
- Ma, R., Liang, W., Sun, Q., Qiu, X., Lin, Y., Ge, X., Jueraitetibaike, K., Xie, M., Zhou, J., Huang, X., Wang, Q., Chen, L., 2018. Sirt1/Nrf2 pathway is involved in oocyte aging by regulating Cyclin B1. Aging (Albany NY) 10 (10), 2991–3004. https://doi.org/ 10.18632/aging.101609.

- Michan, S., Li, Y., Chou, M.M., Parrella, E., Ge, H., Long, J.M., Allard, J.S., Lewis, K., Miller, M., Xu, W., Mervis, R.F., Chen, J., Guerin, K.I., Smith, L.E., McBurney, M.W., Sinclair, D.A., Baudry, M., de Cabo, R., Longo, V.D., 2010. SIRT1 is essential for normal cognitive function and synaptic plasticity. J. Neurosci. 30 (29), 9695–9707. https://doi.org/10.1523/JNEUROSCI.0027-10.2010.
- Min, S.W., Cho, S.H., Zhou, Y., Schroeder, S., Haroutunian, V., Seeley, W.W., Huang, E.J., Shen, Y., Masliah, E., Mukherjee, C., Meyers, D., Cole, P.A., Ott, M., Gan, L., 2010. Acetylation of tau inhibits its degradation and contributes to tauopathy. Neuron 67 (6), 953–966. https://doi.org/10.1016/j.neuron.2010.08.044.
- Murphy, K., Llewellyn, K., Wakser, S., Pontasch, J., Samanich, N., Flemer, M., Hensley, K., Kim, D.S., Park, J., 2018. Mini-GAGR, an intranasally applied polysaccharide, activates the neuronal Nrf2-mediated antioxidant defense system. J. Biol. Chem. 293 (47), 18242–18269. https://doi.org/10.1074/jbc.RA117.001245.
- Pajares, M., Jimenez-Moreno, N., Garcia-Yague, A.J., Escoll, M., de Ceballos, M.L., Van Leuven, F., Rabano, A., Yamamoto, M., Rojo, A.I., Cuadrado, A., 2016. Transcription factor NFE2L2/NRF2 is a regulator of macroautophagy genes. Autophagy 12 (10), 1902–1916. https://doi.org/10.1080/15548627.2016.1208889.
- Plant, L.D., Boyle, J.P., Smith, I.F., Peers, C., Pearson, H.A., 2003. The production of amyloid beta peptide is a critical requirement for the viability of central neurons. J. Neurosci. 23 (13), 5531–5535. https://doi.org/10.1523/JNEUROSCI.23-13-05531.2003
- Puzzo, D., Privitera, L., Leznik, E., Fa, M., Staniszewski, A., Palmeri, A., Arancio, O., 2008. Picomolar amyloid-positively modulates synaptic plasticity and memory in Hippocampus. J. Neurosci. 28 (53), 14537–14545. https://doi.org/10.1523/ JNFUROSCI.2692-08.2008.
- Rottkamp, C.A., Raina, A.K., Zhu, X., Gaier, E., Bush, A.I., Atwood, C.S., Chevion, M., Perry, G., Smith, M.A., 2001. Redox-active iron mediates amyloid-beta toxicity. Free Radic. Biol. Med. 30 (4), 447–450. https://doi.org/10.1016/s0891-5849(00)00494-
- Shin, J.W., Kwon, S.B., Bak, Y., Lee, S.K., Yoon, D.Y., 2018. BCI induces apoptosis via generation of reactive oxygen species and activation of intrinsic mitochondrial pathway in H1299 lung cancer cells. Sci. China Life Sci. 61 (10), 1243–1253. https:// doi.org/10.1007/s11427-017-9191-1.
- Theurey, P., Connolly, N.M.C., Fortunati, I., Basso, E., Lauwen, S., Ferrante, C., Moreira Pinho, C., Joselin, A., Gioran, A., Bano, D., Park, D.S., Ankarcrona, M., Pizzo, P., Prehn, J.H.M., 2019. Systems biology identifies preserved integrity but impaired metabolism of mitochondria due to a glycolytic defect in Alzheimer's disease neurons. Aging Cell 18 (3), e12924. https://doi.org/10.1111/acel.12924.
- Varadarajan, S., Kanski, J., Aksenova, M., Lauderback, C., Butterfield, D.A., 2001. Different mechanisms of oxidative stress and neurotoxicity for alzheimer's aβ(1–42) and aβ(25–35). J. Am. Chem. Soc. 123 (24), 5625–5631. https://doi.org/10.1021/ia010452r.
- Vassar, R., Bennett, B.D., Babu-Khan, S., Kahn, S., Mendiaz, E.A., Denis, P., Teplow, D.B., Ross, S., Amarante, P., Loeloff, R., Luo, Y., Fisher, S., Fuller, J., Edenson, S., Lile, J., Jarosinski, M.A., Biere, A.L., Curran, E., Burgess, T., Louis, J.C., Collins, F., Treanor, J., Rogers, G., Citron, M., 1999. Beta-secretase cleavage of Alzheimer's amyloid precursor protein by the transmembrane aspartic protease BACE. Science 286 (5440), 735–741. https://doi.org/10.1126/science.286.5440.735.
- Yen, J.-H., Wu, P.-S., Chen, S.-F., Wu, M.-J., 2017. Fisetin protects PC12 cells from tunicamycin-mediated cell death via reactive oxygen species scavenging and modulation of Nrf2-Driven gene expression, SIRT1 and MAPK signaling in PC12 cells. Int. J. Mol. Sci. 18 (4), 852. https://doi.org/10.3390/ijms18040852.
- Zhang, J., Cheng, Y., Gu, J., Wang, S., Zhou, S., Wang, Y., Tan, Y., Feng, W., Fu, Y., Mellen, N., Cheng, R., Ma, J., Zhang, C., Li, Z., Cai, L., 2016. Fenofibrate increases cardiac autophagy via FGF21/SIRT1 and prevents fibrosis and inflammation in the hearts of Type 1 diabetic mice. Clin. Sci. 130 (8), 625–641. https://doi.org/10.1042/CS20150623
- Zhang, Z., Shen, Q., Wu, X., Zhang, D., Xing, D., 2020. Activation of PKA/SIRT1 signaling pathway by photobiomodulation therapy reduces  $A\beta$  levels in Alzheimer's disease models. Aging Cell 19 (1), e13054. https://doi.org/10.1111/acel.13054.
- Zhao, Y., Sivaji, S., Chiang, M.C., Ali, H., Zukowski, M., Ali, S., Kennedy, B., Sklyar, A., Cheng, A., Guo, Z., Reed, A.K., Kodali, R., Borowski, J., Frost, G., Beukema, P., Wills, Z.P., 2017. Amyloid Beta peptides block new synapse assembly by nogo receptor-mediated inhibition of T-Type calcium channels. Neuron 96 (2), 355–372. https://doi.org/10.1016/j.neuron.2017.09.041 e6.
- Zheng, T., Lu, Y., 2016. SIRT1 protects human Lens Epithelial cells against oxidative stress by inhibiting p53-Dependent apoptosis. Curr. Eye Res. 41 (8), 1068–1075. https://doi.org/10.3109/02713683.2015.1093641.
- Zhi, W.-H., Zeng, Y.-Y., Lu, Z.-H., Qu, W.-J., Chen, W.-X., Chen, L., Chen, L., 2014. Simvastatin exerts antiamnesic effect in  $A\beta25$ -35-Injected mice. CNS Neurosci. Ther. 20 (3), 218–226. https://doi.org/10.1111/cns.12190.
- Zhu, L., Chi, T., Zhao, X., Yang, L., Song, S., Lu, Q., Ji, X., Liu, P., Wang, L., Zou, L., 2018a. Xanthoceraside modulates neurogenesis to ameliorate cognitive impairment in APP/PS1 transgenic mice. J. Physiol. Sci. 68 (5), 555–565. https://doi.org/ 10.1007/s12576-017-0561-9.
- Zhu, L., Yang, L., Zhao, X., Liu, D., Guo, X., Liu, P., Chi, T., Ji, X., Zou, L., 2018b. Xanthoceraside modulates NR2B-containing NMDA receptors at synapses and rescues learning-memory deficits in APP/PS1 transgenic mice. Psychopharmacology 235 (1), 337–349. https://doi.org/10.1007/s00213-017-4775-6.